



Research article

From waste to solution: Valorisation of a dolomite by-product for degraded soil rehabilitation

Lorena Salgado^{a,b}, José Luis R. Gallego^a, Roberto Caballero^c, María Larramona^a,
Elias Afif^{a,d}, Maximino Herías^e, Raquel Lara^e, Juan María Menéndez-Aguado^f,
Rubén Forján^{f,g,*}

^a Environmental Biogeochemistry & Raw Materials Group, and Institute of Natural Resources and Territorial Planning (INDUROT), University of Oviedo, Mieres, Spain

^b Cartographic, Geodetic, and Photogrammetric Engineering Area, Department of Mining Technology, Surveying, and Structures, University of León, Ponferrada, Spain

^c RC Materials & Processes Consulting EAR, Trinidad, 1, Gijón, Spain

^d Agroforestry Engineering Area, Department of Organisms and Systems Biology, Polytechnic School of Mieres, University of Oviedo, Mieres, Spain

^e INTOCAST IBERICA SL., Av. Conde Santa Bárbara, 12, Lugones, Spain

^f Environmental Biogeochemistry & Raw Materials Group, and Asturias Raw Materials Institute (ASRAM), University of Oviedo, Mieres, Spain

^g GEAPAGE Group and Department of Animal Biology, Parasitology, Soil Science and Agricultural Chemistry, University of Salamanca, Salamanca, Spain

ARTICLE INFO

Keywords:

Soil amendments
Metal(oid) immobilisation
Phytostabilisation
Fertility
Nature-based solutions

ABSTRACT

Acidic, metal(loid)-contaminated soils require scalable circular solutions; the efficacy of a finely milled dolomite by-product, alone or co-applied with vermicompost (VC) or biochar (B), was assessed as amendments to rehabilitate an Iberian mine-impacted soil and to enable phytostabilisation with *Lolium multiflorum*. In a greenhouse pot trial comparing five amended treatments (SD, SV, SB, SVD, SBD) against an unamended control, soil chemistry (pH, C/N, available P, CEC, Al saturation), TCLP-extractable Cu–Zn–As, plant biomass, and multivariate response (PCA) were quantified. Dolomite sharply neutralised acidity (pH 3.1 → 8.3–8.5), increased CEC (23.0 → 65.5–81.9 cmol₍₊₎/kg), and reduced Al saturation (11.2 % → ~0.02 %), with large decreases in TCLP-Cu fell to <10 mg/kg in dolomite-containing treatments and to <3 mg/kg with VC formulations; Zn was suppressed to <65 mg/kg except where liming counteracted B effects. Arsenic showed a distinct pattern: VC increased TCLP-As in close association with available P, whereas dolomite alone or with B kept As below detection—most plausibly via Ca/Mg-driven (co)precipitation of sparingly soluble arsenate/phosphate phases; notably, SVD < SV for As, indicating partial mitigation by dolomite. Vegetation failed in the control but established across all amended soils, with biomass maximized under VC. Overall, the results indicate that dolomite by-product particularly in combination with VC provides a circular, field-relevant route to restore soil function and reduce bioavailable Cu and Zn by >90 % while sustaining plant establishment; given VC-linked As mobilization, co-amendment with Fe-rich sorbents and prudent P management are recommended to minimize risk in practical applications.

1. Introduction

Mining, both historical and ongoing, has played a fundamental role in global economic development, yet it has also resulted in significant environmental degradation, particularly of soil and adjacent ecosystems (Worlanyo and Jiangfeng, 2021). Although remediation efforts typically focus on mining infrastructure (e.g., tailings, waste rock), contamination often extends well beyond these boundaries, affecting agricultural lands,

forests, and aquatic systems (Cañedo-Argüelles et al., 2013; Kossoff et al., 2014; Salgado et al., 2023; Varol, 2011).

Concurrently, the large-scale generation of industrial waste represents a critical environmental challenge. In response, the European Union has implemented stringent policy frameworks such as the Zero Waste initiative and the Circular Economy Strategy that mandate the valorisation of industrial by-products as a central mechanism for environmental sustainability and climate neutrality (European Commission,

* Corresponding author. GEOPAGE Group and Department of Animal Biology, Parasitology, Soil Science and Agricultural Chemistry, University of Salamanca, Salamanca, Spain.

E-mail address: forjanruben@usal.es (R. Forján).

<https://doi.org/10.1016/j.jenvman.2025.127795>

Received 24 September 2025; Received in revised form 17 October 2025; Accepted 24 October 2025

0301-4797/© 2025 The Authors. Published by Elsevier Ltd. This is an open access article under the CC BY-NC license (<http://creativecommons.org/licenses/by-nc/4.0/>).

2014; European Commission, 2020). Among industrial waste streams, residues generated by dolomite processing deserve particular scrutiny, as European production alone surpasses 20 Mt yr⁻¹ (Ursuegüfa et al., 2023). These fines are intensely hygroscopic: upon contact with atmospheric moisture, they hydrate almost instantaneously, causing agglomeration, volumetric expansion and heat release. To avoid operational incidents, producers are compelled to palletise and hermetically wrap the material immediately after generation, a time-consuming and costly practice (Lanas and Alvarez, 2004; Lin et al., 2021). The challenge escalates at landfill, where much larger masses of residue hydrate, well and release strongly alkaline leachates, complicating leachate treatment and jeopardising liner integrity. Consequently, dolomite-derived residues pose a persistent management challenge for producers, waste operators, and landfill managers alike, while imposing significant environmental burdens when disposed of.

Utilising such residues as soil amendments offers a promising strategy for the rehabilitation of degraded soils, especially those characterised by severe acidification and metal contamination. Dolomitic by-products (CaMg(CO₃)₂), rich in Ca²⁺ and Mg²⁺ and with an intrinsic pH > 9, serve as potent liming agents that neutralise soil acidity and facilitate the precipitation of heavy metals as insoluble phases (Islas-Valdez et al., 2017; Rinklebe et al., 2016). Their local reuse avoids the need for virgin limestone extraction, reduces greenhouse gas emissions from transportation and landfilling, and supports circular material flows (Lou and Nair, 2009; Patel et al., 2025).

Nature-based solutions (NBS) provide a practical and integrative framework to simultaneously address soil rehabilitation and waste valorisation by substituting engineering-intensive remediation with biologically driven functions (European Commission, 2017). These strategies incorporate organic amendments (e.g., vermicompost, biochar), inorganic residues (e.g., dolomite by-products), metal-tolerant vegetation, and microbial stimulation to restore soil structure and immobilise contaminants (Song et al., 2019). Organic fractions supply labile carbon and nutrients, while mineral components elevate pH and cation exchange capacity, creating conditions conducive to metal stabilisation. This synergistic approach mitigates erosion, supports vegetation cover, and promotes atmospheric CO₂ capture (Hütsch et al., 2002; Pang and Xu, 2024), contributing to climate change mitigation (Fiorentino et al., 2025; Lenton, 2010). In the same context, phytoremediation, implemented with species such as *Lolium multiflorum*, plays a pivotal role within the NBS framework by promoting vegetation establishment, stabilising contaminants, and enhancing soil productivity (Chalot, 2024; Kafle et al., 2022; Wong, 2003). When combined with organic and inorganic amendments, its efficacy in restoring degraded soils is markedly improved (Baragaño et al., 2021; Fang et al., 2025).

Although dolomitic by-products have been proposed as potential liming agents, systematic research on their performance in soils combining extreme acidity with multi-metal(loid) contamination remains scarce. In particular, the potential synergies between dolomite-derived residues and organic amendments such as vermicompost or biochar are poorly understood, especially regarding their capacity to both immobilise contaminants and restore soil functionality within Nature-Based Solution (NBS) frameworks. Furthermore, field-relevant evaluations that integrate chemical, biological, and structural indicators of remediation success are still limited, which hinders the development of operational guidelines for large-scale implementation.

Despite extensive research on liming agents and organic amendments, the mechanistic and practical benefits of co-applying a finely milled dolomite by-product with vermicompost in highly acidic, metal-impacted soils remain underexplored. This study explicitly evaluates that combined, circular and low-cost strategy, positing that it can outperform single-amendment approaches by coupling rapid acidity neutralization and Ca/Mg supply with organic-matter/nutrient inputs and DOC-mediated sorption processes.

Objective of the study. This work tests the hypothesis that a finely milled dolomitic by-product, applied alone or in combination with

vermicompost or biochar, can concurrently immobilise Cu, Zn, and As, restore key soil physicochemical properties, and support phytostabilisation with *Lolium multiflorum* in a highly acidic, mine-impacted soil from southwestern Spain. To evaluate this integrated objective, changes in the bioavailable fractions of the target metal(loid)s, improvements in pH, soil organic carbon, available nutrients, and cation exchange capacity, and the establishment and stabilising capacity of *L. multiflorum* are quantified, while explicitly assessing how organic co-amendments differentially modulate the behavior of anionic (As) versus cationic (Cu, Zn) contaminants.

2. Material and methods

2.1. Soil and soil sampling

The study area is located on the right bank of a river estuary, within an environment historically influenced by mining activities. Running parallel to the edge of the salt marsh was a former mining railway line, oriented approximately north-south, which was once used for transporting pyrite from the mining basin to a river pier. In the vicinity, a mineral crushing and grinding plant was constructed. Its operations, along with the infilling and stockpiling carried out around the facility and the railway line, have caused significant metal contamination in the area. The analysed samples originate from the surroundings of these pyrite storage and fill zones. Although the area is situated within a salt marsh, it is not directly affected by tidal fluctuations, and the soil exhibits medium permeability. For confidentiality reasons related to the participation of a private company, the exact site coordinates are not reported. The characteristics of the soil selected for this experiment are detailed in Table S1 (see analytical methods in section 2.4).

2.2. Amendments

Vermichar Lombricompost S.L. supplied biochar (B) and vermicompost (VC). B is obtained by pyrolysis of oak wood at 500. At the same time, vermicompost is the result of decomposing mushroom substrate and cereal crop residues, facilitated by earthworms of the *Eisenia fetida* specie. In contrast, vermicompost is the result of decomposing mushroom substrate and cereal crop residues, facilitated by the *Eisenia fetida* species of earthworms. The general characteristics of the biochar and vermicompost used are presented in Table S1.

The INTOCAST plant in Lugones, Spain, provided the dolomite by-product. These hydrated dolomite fines are produced during the conventional grinding of dolomite sinter. The dolomite-grinding unit at the INTOCAST plant in Lugones (Asturias, Spain) operates a closed-loop dust-collection system in which the dust generated during sinter processing is continuously extracted, filtered, and discharged into a storage silo. A fraction of this material is recycled in the mixing facility and incorporated into the dolomite-brick pressing mixes; nevertheless, a net excess of approximately 50–60 tons per year remains. This surplus is stored in stretch-wrapped big bags to prevent—or at least delay—further hydration.

In addition to the baseline properties of the dolomite by-product summarised in Table S1, more detailed analyses were conducted on the dolomite by-product, as it represents the most novel amendment investigated in this study. Laser-diffraction analysis (Beckman-Coulter LS Particle Size Analyser) performed in accordance with ISO 13320 (International Organization for Standardization, 2020) on the dolomite subproduct yielded a broad yet unimodal particle-size distribution: D10 = 1.372 μm, D50 = 8.882 μm and D90 = 42.49 μm, giving a span (D90–D10)/D50 of 4.6. Hence, 50 % of the material lies within the <9 μm silt–clay fraction, providing a high specific surface area and potential geo-reactivity, while the absence of particles >60 μm reduces segregation during blending and application in soil-remediation trials.

Powder X-ray diffraction (XRD) was performed on the dolomite by-product using a Philips X'Pert PRO diffractometer equipped with a Cu-

K α tube ($\lambda = 1.54060 \text{ \AA}$, 40 kV, 45 mA, 240 mm goniometer radius). Scans were collected from 5.0° to 79.9° 2θ with a 0.017° step size and 90s counting time per step under ambient conditions (25°C). Diffractograms were processed with X'Pert HighScore Plus and semi-quantified by the RIR method in X-Powder™, giving $39.0 \pm 6.9 \text{ wt\%}$ periclase (MgO), $37.9 \pm 0.9 \text{ wt\%}$ portlandite (Ca(OH)_2), $8.8 \pm 0.7 \text{ wt\%}$ brucite (Mg(OH)_2), $4.4 \pm 0.7 \text{ wt\%}$ calcite (CaCO_3) and $\approx 10 \text{ wt\%}$ amorphous material (Fig. 1A). Complementary thermogravimetric analysis (TGA, TGA/SDTA851e) of the same material, carried out in the University of Oviedo analytical services, provided mass-loss profiles that corroborate the dehydration of hydroxides and the decarbonation of residual carbonate identified by XRD, thereby constraining the thermal stability window of the sub-product for subsequent soil-remediation trials (Fig. 1B).

2.3. Greenhouse experiment and plant growth

The experimental design consisted of five soil treatments, with the control soil prepared under controlled conditions (average temperature of 15°C and 70 % humidity). The unamended control (S) consisted solely of the degraded soil. Amendment treatments included: soil mixed with the dolomite by-product (SD), soil amended with vermicompost (SV), soil amended with biochar (SB), soil receiving a combined addition of the dolomite by-product and vermicompost (SVD), and soil receiving the dolomite by-product together with biochar (SBD). Amendment percentages for each treatment are detailed in Table 1. All treatments, including the control, were prepared in triplicate ($n = 3$), thoroughly homogenised, transferred to 1 L plastic pots, and subsequently vegetated under greenhouse conditions as described below.

The selected proportions are reproducible at pilot and field scales because the dolomite by-product is readily available and vermicompost is a cost-effective amendment that even mining companies or public administrations can produce autonomously. Moreover, the effectiveness

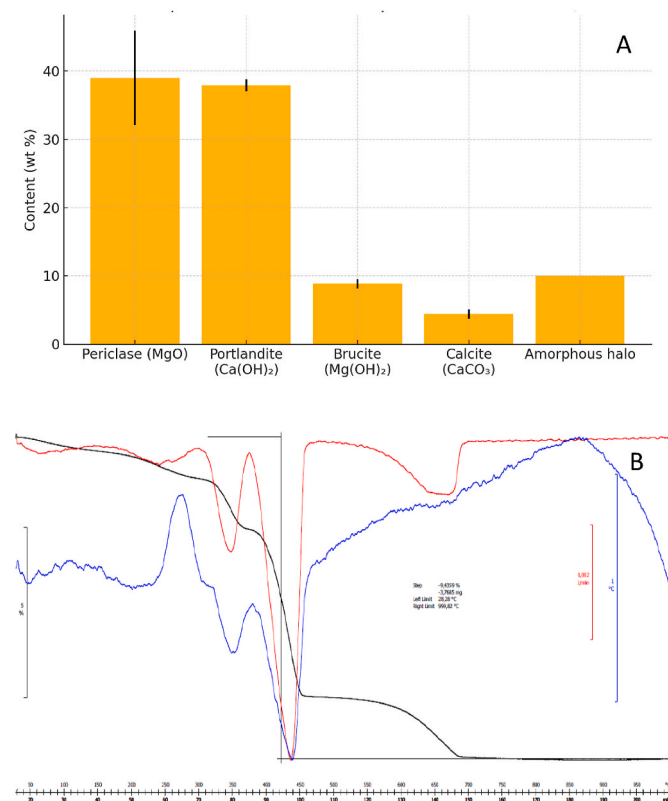


Fig. 1. A: X-ray diffractometric study (semi-quantitative phase Composition). B: Thermogravimetric analysis.

Table 1

Proportions (%) and conditions used in controls and the different treatments.

Code	Polluted soil	Dolomite by-product	Vermicompost	Biochar
S	100			
SD	98	2		
SV	85		15	
SB	95			5
SVD	83	2	15	
SBD	93	2		5

S = contaminated soil (negative control); SD = S + Dolomite by-product; SV = S + vermicompost; SB = S + biochar; SVD = S + vermicompost + dolomite by-product; SBD = S + biochar + dolomite by-product.

of biochar in contaminated soils is well documented, and a 5 % application rate is sufficient to elicit measurable effects (Forján et al., 2018).

After 15 days of incubation with deionised water at field capacity, ryegrass seeds (*Lolium multiflorum*) provided by Zoonort S.L. (Lugo, Spain), were sown (1.5 g per pot). The soils were watered to maintain field capacity throughout the experiment. Ryegrass growth was evaluated over a 45-day period. Afterwards, the plants were harvested, and samples were collected.

Soil samples were homogenised and separated according to the type of analysis. For the physicochemical analysis, the samples were air-dried and sieved through a 2 mm mesh, while for biological analysis, they were only sieved (<2 mm) and kept fresh (4°C).

2.4. Soil and amendments characterisation

The bulk density was measured using a steel cylinder with known dimensions. Pseudototal metal concentrations were obtained by microwave-assisted aqua regia digestion (ETHOS 1, Milestone) and quantified by inductively coupled plasma optical emission spectrometry (ICP-OES; Optima 4300 DV, PerkinElmer). The potentially mobile metal fraction was assessed with the Toxicity Characteristic Leaching Procedure (TCLP) (USEPA, 1992). Soil pH was measured in a 1:2.5 soil-to-water suspension using a combined glass electrode (Porta, 1986). Total carbon and total nitrogen were determined on finely ground samples with a LECO CN-2000 combustion analyser, and the organic matter content and organic carbon content were calculated from TC by the conventional Van Bemmelen factor (1.724) (Van Bemmelen, 1890). Plant-available phosphorus (P) was extracted with the Mehlich solution (Mehlich, 1984). Exchangeable Ca^{2+} , K^+ , Mg^{2+} , Na^+ and Al^{3+} were released with 0.1 M BaCl_2 (Hendershot and Duquette, 1986) and measured on the same ICP-OES system; effective cation-exchange capacity (CEC) was taken as the sum of these cations (Houba et al., 2008).

The aluminium saturation (Als_{at}) was subsequently calculated as:

$$\text{Als}_{at} = \frac{\text{Exchangeable Al}^{3+}}{\text{CEC}} \times 100$$

The exchangeable sodium percentage (ESP) was subsequently calculated as (Forján et al., 2024):

$$\text{ESP} = \frac{\text{Exchangeable Na}^+}{\text{CEC}} \times 100$$

2.5. Soil organic carbon stocks (SOCS)

To estimate soil organic carbon stocks, the protocol proposed by Anta et al. (2015) has been followed. The equation and parameters used in the stock calculation are detailed below:

$$\text{Soil organic carbon stocks} = \% \text{ OC} \times \text{BD} \times [1 - (\text{VG}/100)] \times \text{LT}$$

Soil organic carbon stocks: total amount of soil organic carbon to given depth (tC ha^{-1}); OC: soil organic carbon content for given depth; BD: dry bulk density (g cm^{-3}); VG: volume of gravels; LT: thickness of soil layer (cm).

2.6. Factors for plant production

A series of critical values was assigned to each of the chemical parameters, based on the model of the SFCC (Soil Fertility Capability Classification) proposed by, and adapted by Calvo et al. (1987); Macías Vázquez and Calvo de Anta (1983) and Hazelton and Murphy (2007). These were used to evaluate the limiting factors for plant production.

- Factor c when the pH < 3.5. Factor c refers to conditions of extreme soil acidity, characterised by pH values lower than 3.5. This condition is critical for the development of most plant species, as it directly affects both the availability of nutrients and the toxicity of certain elements.
- K factor indicates that a soil is K-deficient if $K^+ < 0.2 \text{ cmol}_{(+)} / \text{kg}$.
- Mg Factor (Mg deficiency): this factor applies to soils where the level of available Mg^{2+} is not sufficient for the needs of the plants, which may be caused either by a low content of this element in the exchange complex ($< 0.4 \text{ cmol}_{(+)} / \text{kg}$ or by an imbalance in the $\text{Ca}^{2+} / \text{Mg}^{2+}$ ratio > 50).
- Ca Factor (Ca deficiency): when the value of the Ca^{2+} content in the exchange complex is $< 1.5 \text{ cmol}_{(+)} / \text{kg}$.
- Na Factor: The Na Factor is defined as the condition wherein Na saturation within the 50 cm surface exchange complex reaches or exceeds 15 %.

2.7. Plant analysis

The plants were harvested at 180 days. Fresh biomass was weighed immediately, and dry mass was assessed after oven-drying for 48 h at 80 °C. The dry mass was then ground in a cryogenic mill with liquid nitrogen (6775 Freezer/Mill® SPEX SamplePrep) before metal analysis, which consisted of acid digestion of a subsample (0.2 mg) with 8 ml H_2O_2 , 6 ml HNO_3 , and 2 ml HCl in a hot plate in a Teflon bomb (90 min, 150 °C) (Cerdeira-Pérez et al., 2019; Gebrekidan et al., 2013; Rosenkranz et al., 2019). Metal concentrations in the supernatant were determined by ICP-AES (Optima 4300 DV; PerkinElmer).

The bioconcentration factor (BF) describes the ratio of available metal(loid) concentration that is taken up into shoots. High BF values indicate a high concentration of elements in shoots compared to the available concentration of the metal(loid)s (Rodríguez-Vila et al., 2015).

2.8. Data analysis

All analytical determinations were performed in triplicate. A statistical analysis was conducted to verify whether there were statistically significant differences in the parameters analysed between the soil and the various treatments across multiple treatments. The data obtained were statistically treated using the SPSS program version 24.0 for Windows. Analysis of variance (ANOVA) and test of homogeneity of variance were carried out. In the case of homogeneity, a post hoc least significant difference (LSD) test was performed. When there was no homogeneity, Dunnett's T3 test was performed. A correlated bivariate analysis was also conducted using Pearson correlation. To carry out a principal component analysis (PCA), the TCLP-metal concentrations were natural-log transformed, all variables were autoscaled ($z = 0, \sigma = 1$), and a PCA was calculated on the correlation matrix using the SVD routine of scikit-learn 1.4 under Python 3.10.

3. Results and discussion

3.1. General results

3.1.1. Bulk density

The control soil (S) exhibited the highest bulk density, 1.34 g cm^{-3} , a value typically associated with medium-textured soils of relatively loose

structure (Table 2). All amendments lowered this density; notably, the organic amendments combined with the dolomite by-products (SBD, SVD) produced the most significant reduction (Table 2).

Bulk density dropped to 1.10 g cm^{-3} with the SBD treatment and to 1.13 g cm^{-3} with SVD (Table 2). Authors such as Sweet et al. (2025) or Verheijen et al. (2019) have demonstrated that the application of organic amendments can reduce soil bulk density; this reduction is beneficial because it signifies a substantial improvement in soil structure, thereby placing the soil within a physically optimal range for most crop species (Garbuz et al., 2021).

3.1.2. Changes in pH values

First, it must be emphasised that soil S is constrained by Factor c for plant production, given that its pH is below 3.5 (Table 2). All treatments produced a significant rise in the pH of soil S (Table 2) and thereby ceased to be constrained by Factor c. Biochar addition (SB), despite its intrinsic pH of 9.44, caused only a slight but statistically significant increase, presumably because of the relatively low application rate (Table 2).

The highest pH values were recorded after the direct incorporation of the dolomite by-product (SD), vermicompost (SV), or their combined application (SVD) (Table 2). Moreover, the mixture of the dolomite by-product with biochar (SBD) yielded a pH significantly higher than that obtained with the biochar alone (SB), underscoring the strong liming capacity of the dolomite by-product.

The pH-neutralising capacity of the dolomite by-product stems from its composition, which contains approximately 40 % periclase (MgO) and approximately 40 % portlandite [$\text{Ca}(\text{OH})_2$] (Fig. 1A), two phases with very high neutralising power that can rapidly raise soil pH. Portlandite is moderately soluble and releases OH^- as soon as it hydrates, driving the soil solution towards a pH of 12–12.5; liming trials with $\text{Ca}(\text{OH})_2$ have reported pH increases of up to 12.3 under experimental conditions, corroborating its strong alkalinising effect (Martin et al., 2024). Periclase hydrates more slowly to $\text{Mg}(\text{OH})_2$. However, $\text{Mg}(\text{OH})_2$ is less soluble than portlandite; it is, however, sufficiently soluble to maintain pH values of 10–11 for extended periods, thereby acting as a slow-release alkaline buffer (Kameda et al., 2018). Because each mole of $\text{Ca}(\text{OH})_2$ or $\text{Mg}(\text{OH})_2$ neutralises two protons (H^+), a mixture containing 40 % of each oxide/hydroxide has a theoretical neutralising value about 1.5 times greater than that of agricultural lime (CaCO_3), which explains the rapid and pronounced pH increase observed when the by-product is incorporated into acidic soils.

Several studies, such as those by Wang et al. (2021), have recorded a pH rise after vermicompost is incorporated into soils. During vermicomposting, the calciferous glands of earthworms secrete CaCO_3 micro-aggregates that remain embedded in the final vermicompost. Mineralisation of the organic matrix also releases base cations (Ca^{2+} , Mg^{2+} , K^+ , Na^+) originating from the ash fraction of plant and animal residues. Once added to the exchange complex, these cations displace H^+ and Al^{3+} from colloidal surfaces, increasing base saturation and, consequently, soil pH (García-Montero et al., 2013). As shown in Table S1, the vermicompost used in this study is rich in Ca and Mg. In the present study, soil pH exhibited a robust positive correlation with exchangeable Ca^{2+} ($r = 0.98, p < 0.01$), a strong positive correlation with exchangeable Mg^{2+} ($r = 0.90, p < 0.01$), and a strong positive correlation with exchangeable Mg^{2+} ($r = 0.90, p < 0.01$). In addition, the carboxylic and phenolic functional groups of its humic substances deprotonate progressively: at low pH they remain largely undissociated, whereas, as pH rises, they release H^+ , providing substantial buffering capacity and preventing extreme fluctuations (Masini et al., 1998).

The rise in soil pH induced by biochar amendments in acidic soils has been documented in numerous studies (Forján et al., 2024; Rúa-Díaz et al., 2023). Biochar raises the pH of acidic soils through a combination of rapid “liming” and slower buffering processes (Bolan et al., 2023). During pyrolysis, part of the feedstock's mineral fraction is transformed into carbonates, bicarbonates, and oxides/hydroxides of Ca, Mg, K, and

Table 2
Results of general soil properties and the different treatments after the experimental period.

		S	SD	SB	SV	SBD	SVD
Bulk density	g/cm ³	1.34 ± 0.07a	1.22 ± 0.01b	1.21 ± 0.04b	1.16 ± 0.02bc	1.10 ± 0.06c	1.13 ± 0.02c
pH		3.13 ± 0.05d	8.30 ± 0.18a	3.88 ± 0.12c	8.46 ± 0.11a	6.70 ± 0.11b	8.35 ± 0.01a
OC	%	0.46 ± 0.03c	0.49 ± 0.01c	5.29 ± 0.16 ab	6.00 ± 0.84a	4.66 ± 0.98b	4.58 ± 0.02b
N	%	0.04 ± 0.01c	0.04 ± 0.01c	0.09 ± 0.01b	0.44 ± 0.03a	0.09 ± 0.01b	0.30 ± 0.00a
C/N		11.10 ± 1.91b	13.76 ± 4.48b	55.28 ± 8.39a	13.68 ± 1.96b	50.00 ± 3.51a	15.00 ± 0.49b
P	mg/kg	0.13 ± 0.01c	0.14 ± 0.01c	0.53 ± 0.04c	26.54 ± 1.42a	0.22 ± 0.01c	15.39 ± 0.28b
Ca+2	cmol(+)/kg	12.35 ± 1.65d	46.35 ± 3.70b	15.82 ± 2.23d	35.71 ± 1.34c	51.99 ± 0.11a	54.54 ± 0.20a
Mg+2		2.80 ± 0.50bc	13.18 ± 0.81a	1.87 ± 0.54c	4.39 ± 0.57b	13.44 ± 1.01a	15.62 ± 0.16a
Na+		5.23 ± 0.91a	5.34 ± 0.14a	3.35 ± 0.93a	4.75 ± 0.51a	6.24 ± 0.51a	5.52 ± 1.35a
K+		0.03 ± 0.01d	0.62 ± 0.02c	0.22 ± 0.05d	2.86 ± 0.01b	0.87 ± 0.12c	3.43 ± 0.40a
Al+3		2.61 ± 0.71a	0.01 ± 0.00c	0.61 ± 0.05b	0.01 ± 0.00c	0.02 ± 0.00c	0.02 ± 0.00c
CEC		23.02 ± 2.39c	65.52 ± 4.41 ab	22.02 ± 3.59c	47.74 ± 0.41b	70.56 ± 4.29a	81.92 ± 3.35a
Alsat	%	11.23 ± 2.14a	0.02 ± 0.00c	3.34 ± 0.50b	0.02 ± 0.00c	0.02 ± 0.00c	0.02 ± 0.00c
EPS		22.73 ± 3.08aa	8.18 ± 0.51c	15.12 ± 2.86b	9.96 ± 1.10c	8.87 ± 0.99c	6.76 ± 1.78c

S = contaminated soil (negative control); SD = S + Dolomite by-product; SV = S + vermicompost; SB = S + biochar; SVD = S + vermicompost + dolomite by-product; SBD = S + biochar + dolomite by-product. For each row, different letters in different samples mean significant differences (n = 3, ANOVA; P < 0.05). Typical deviation is represented by ±

Na that concentrate in the biochar ash (Arwenyo et al., 2023). When this ash comes into contact with soil moisture, it dissolves, consumes H⁺, and releases basic cations that replace H⁺ and Al³⁺ on exchange sites, thereby increasing base saturation and driving the soil solution pH upward (Geng et al., 2022). Simultaneously, negatively charged functional groups on the biochar surface (carboxylate, phenolate) complex hydroxy-Al species and adsorb protons, further mitigating acidity. Because biochar particles are highly porous and persist for decades, these reactions continue gradually after the initial application, providing sustained pH buffering and limiting re-acidification (Liu et al., 2025).

3.1.3. Organic carbon (OC), total nitrogen (N) and the ratio C/N

Consistent with expectations, incorporation of the dolomite by-product (inorganic amendment, D) into soil S did not result in a statistically significant change in OC content (Table 2). The largest increase in OC was obtained with the vermicompost treatment (SV) and the biochar treatment (SB), followed by the vermicompost + D treatment (SVD) and, lastly, the biochar + D treatment (SBD) (Table 2).

This increase in OC caused by the organic amendments is logical since both biochar and vermicompost had a much higher OC content than S and D (Table S1). The vermicompost introduces a large mass of readily decomposable organic matter: even at moderate rates, it adds several-fold more total organic C per kilogram of soil than the baseline, which is why vermicompost consistently produces the most significant OC gains in field and pot trials (Przemieniecki et al., 2021). The biochar contributes highly condensed, aromatic C that is resistant to mineralisation. Although its application rate may be lower on a mass basis, its C concentration is 60–90 %, so the absolute C addition is still substantial. Long-term trials (>10 years) show net SOC increases of 15–40 % with biochar alone (Ding et al., 2023).

On the other hand, dolomite by-product (D) is almost entirely inorganic (Table S1); when it is co-applied with an organic amendment, it dilutes the dose of added carbon and, through its liming action (Ca²⁺/Mg²⁺), stimulates mineralisation of native soil OC. Laboratory incubations with dolomite have recorded CO₂ releases 3–49 % higher than the control and faster first-order decay constants, confirming this priming effect. Multi-year field trials likewise show that plots amended solely with dolomite can lose OC relative to untreated plots (Wu et al., 2021). In addition, in SVD, the carbon source is vermicompost, which contains labile carbon and microbial biomass that can quickly replenish any liming-induced losses; thus, net OC still rises noticeably (Terefe et al., 2024). In SBD, the carbon source is biochar. Biochar is chemically recalcitrant and less prone to microbial turnover; however, its particulate nature means there are fewer fresh substrates to offset the priming triggered by dolomite. The combined treatment therefore shows the

smallest net gain, reflecting a dilution by D and enhanced mineralisation of native OC without an equivalent influx of labile C (Singh and Cowie, 2014).

As with OC, the addition of dolomite by-product to the soil did not cause a significant change in N content (Table 2). The application of vermicompost, either on its own (SV) or in combination with D (SVD), resulted in a larger increase in N than biochar, whether applied alone (SB) or together with D (SBD) (Table 2). As shown in Table S1, the vermicompost had an N content of 24.35 g/kg, compared to 9.60 mg/kg for biochar, values significantly higher than those reported by S (0.40 g/kg) and D (0.58 g/kg). This response can be attributed to the fact that vermicompost delivers a markedly higher load of organic nitrogen proteins, amino acids and exchangeable NH₄⁺ along with an active microbial biomass that triggers rapid mineralisation; recent trials report 25–95 % increases in total soil N at only moderate vermicompost rates (Malal et al., 2024). Biochar, by contrast, contains very little N (≤1 %) and its carbon is highly aromatic, so it introduces only minimal new nitrogen into the system (de Oliveira Paiva et al., 2024).

Regarding the C/N ratio, the values of SB and SBD stand out (Table 2). The extraordinary C/N ratios observed in the biochar treatments (SB ≈ 55 and SBD ≈ 50) stem from the intrinsic chemistry of biochar and its post-application interactions with soil. Pyrolysis volatilizes most feedstock nitrogen (as NH₃, HCN, and NO_x), leaving a solid that is 60–90 % aromatic carbon but ≤1 % total N (de Oliveira Paiva et al., 2024); the resulting influx of recalcitrant carbon therefore dilutes the existing soil N pool. Subsequent microbial colonisation of char surfaces immobilises additional mineral N to satisfy biomass synthesis and the slow oxidation of residual labile C, further widening the C/N ratio (Phillips et al., 2022). In the SBD treatment, co-applied dolomitic lime elevates pH, enhancing NH₃ volatilisation and reinforcing the relative depletion of nitrogen. Collectively, these processes account for the markedly higher C/N values recorded in soils amended with biochar compared with those receiving vermicompost.

3.1.4. Available phosphorus (P)

Although the biochar amendment yielded the highest measured concentration of P (Table S1), only the treatments incorporating vermicompost (SV, SVD) produced a statistically significant increase in P relative to both the unamended soil (S) and the other treatments (SD, SB, SBD) (Table 2). These findings may be explained, first, by the higher application rate of vermicompost compared with biochar (Sarma et al., 2018) and, second, by the higher proportion of labile organic carbon fractions in vermicompost, which facilitates P mobilisation. For example, dissolved organic carbon competes for P sorption sites and lowers the soil's surface charge, thereby reducing P fixation and increasing the bioavailable P fraction (Wang et al., 2024). Consistently,

a statistically significant positive correlation was detected between P concentration and OC in the SV and SVD treatments ($r = 0.87$, $p < 0.01$).

3.1.5. Cations and cation exchange capacity (CEC)

All treatments except SB (soil + biochar) produced a statistically significant increase in CEC relative to the control soil (Table 2). The highest increases occurred in SD, SBD, and SVD, confirming the contribution of the dolomite by-product (Table 2). This is evidenced by the concomitant rise in Ca^{2+} and Mg^{2+} concentrations in the treatments that received this amendment (SD, SBD, SVD). Moreover, every treatment significantly lowered aluminium saturation and sodicity (ESP) (Table 2). The reduction in aluminium saturation can be attributed to the pH elevation induced by the amendments; indeed, the present study documents a strong inverse correlation between aluminium saturation and soil pH ($r = -0.79$, $p < 0.01$). Furthermore, the Ca^{2+} and Mg^{2+} supplied by the dolomite enlarge the cation exchange complex, thereby displacing exchangeable Al^{3+} and contributing to the observed decline in aluminium saturation (Ingvar Nilsson et al., 2001).

Conversely, soil S was initially constrained by the K Factor, but this constraint disappeared after the various treatments were applied. The Mg Factor or the Ca Factor influenced neither the untreated soil S nor any of the amended soils. Moreover, although soil S exhibits very high sodicity, it does not surpass the threshold that defines the Na Factor.

3.2. Changes in the available Cu, Zn and As concentrations

3.2.1. Copper (Cu)

All treatments applied to soil S markedly decreased the available Cu concentration (Fig. 2A). Although the magnitude of the reduction was statistically equivalent across treatments, the SV and SVD amendments induced the highest declines, lowering extractable Cu by 91 % and 89 %, respectively. The decrease is partly attributable to the pH increase by the amendments in soil S; in fact, pH and extractable Cu exhibited a significant negative correlation (-0.68 , $p < 0.01$) in this study. It is well established that, as soil pH rises, the mobility of metallic cations generally diminishes (Forján et al., 2018a).

In addition, in the case of SD treatment, the dolomitic residue neutralised soil acidity, precipitating Cu as amorphous hydroxide/carbonate phases and sharply lowering solution activity (Vrinceanu et al., 2019). The effectiveness of biochar in reducing bioavailable Cu arises from the combined action of three complementary mechanisms: the

dissolution of its alkaline ash, which consumes H^+ ions, increases soil pH, and promotes the precipitation of Cu as basic hydroxide-carbonates; the presence of abundant carboxyl, hydroxyl, and π -electron-rich sites on the biochar matrix, which enable the formation of strong inner-sphere complexes with Cu; and the high porosity of the material along with biochar-induced micro-aggregation, both of which expand the reactive surface area available for Cu sorption (Ahmad et al., 2014). Vermicompost immobilises Cu primarily through a combination of mechanisms: its humified organic matrix provides a high density of carboxylate and phenolate functional groups that chelate Cu^{2+} into stable, non-exchangeable organo-metallic complexes; the amendment moderately increases pH and contributes Ca^{2+} and Mg^{2+} ions, which facilitate the precipitation of basic Cu hydroxide carbonates; polysaccharides excreted by earthworms enhance micro-aggregation, physically trapping Cu within intra-aggregate pores; and the stimulation of microbial activity under vermicompost application promotes redox-mediated transformations that further reduce the bioavailable Cu fraction (Trentin et al., 2019). The SBD and SVD treatments are combinations of the above treatments, so their positive effects on reducing Cu availability are a result of their combined effects.

3.2.2. Zinc (Zn)

The treatments differed markedly in their effects on extractable Zn concentrations (Fig. 2B). The SBD treatment did not lower available Zn, and SD produced only a slight decline (Fig. 2B). This weak response reflects the cation-exchange hierarchy imposed by the dolomitic amendment: the large influx of Ca^{2+} and Mg^{2+} preferentially displaces Cu^{2+} (which forms highly stable inner-sphere complexes) while exerting little control over Zn^{2+} , whose affinity for exchange sites is similar to that of Ca^{2+} (Mesquita and Vieira E Silva, 1996). Consequently, the increase in CEC alone was insufficient to transfer Zn into non-labile pools (Vrinceanu et al., 2019), and the dolomite residue counteracted the Zn immobilising capacity of biochar, preventing any substantial reduction in extractable Zn (Fig. 2B). By contrast, the most significant decrease occurred when vermicompost was co-applied with dolomite (SVD) (Fig. 2B). Vermicompost supplies humic fractions rich in carboxylate and phenolate groups that chelate Zn^{2+} into stable inner-sphere complexes and, together with the pH rise induced by the amendment, promote precipitation of Zn hydroxide carbonates. Simultaneously, the dolomitic residue enlarges the exchange pool; once the additional sites are saturated with Ca^{2+} and Mg^{2+} , Zn^{2+} is competitively

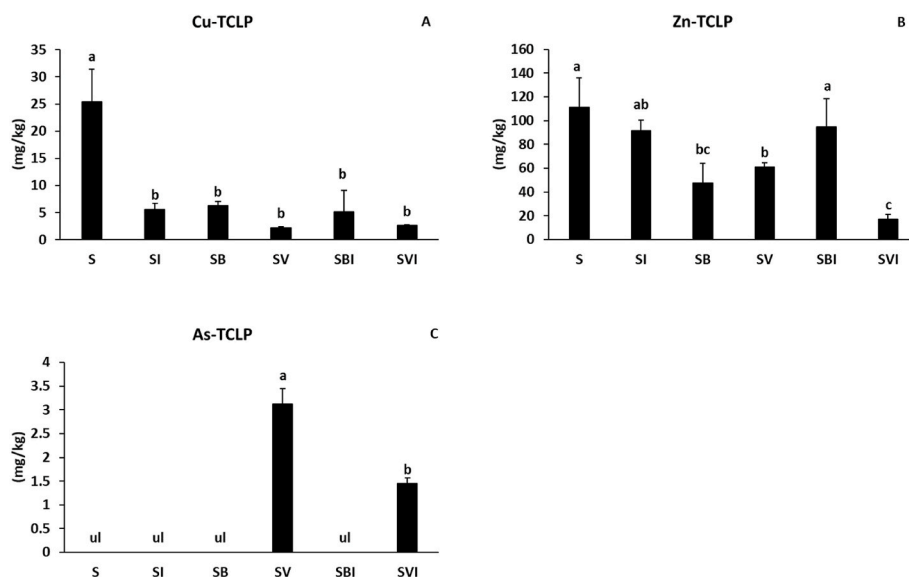


Fig. 2. Changes in Cu (A), Zn (B), and As (C) concentrations following the application of treatments to soil S. Different letters in different samples indicate significant differences ($n = 3$, ANOVA; $p < 0.05$). ul: under detection limit. Error bars represent standard deviation.

displaced and subsequently sequestered by these organic ligands or coprecipitated under the elevated pH (Chunwichit et al., 2024; Formentini et al., 2025).

3.2.3. Arsenic (As)

In soil S (Fig. 2C), As is immobilised because the low pH promotes strong protonation of Fe/Al (hydr)oxide surfaces, enabling the formation of bidentate inner-sphere complexes with As(V) (Arai et al., 2001; Ladeira and Ciminelli, 2004; Waychunas et al., 1993). The same mechanism operates in SB (Fig. 2C), as the biochar fraction is too small to significantly alter the surface charge or pH. In SD and SBD, the dolomitic residue increases pH, yet extractable As remains below the detection limit; this is most plausibly explained by $\text{Ca}^{2+}/\text{Mg}^{2+}$ supersaturation that drives the precipitation of sparingly soluble phases such as $\text{Ca}_3(\text{AsO}_4)_2 \cdot \text{H}_2\text{O}$, thereby curbing As mobility once again (Moon et al., 2004). By contrast, treatments containing vermicompost (SV, SVD) enhanced As mobility (Fig. 2C); this effect is governed. Consistently, a highly significant positive correlation was observed between extractable As and available P (0.99; $p < 0.01$). In this study, the increase in As mobility can be ascribed to the release of labile orthophosphate by the vermicompost at concentrations high enough to saturate the $\equiv \text{FeOH}$ and $\equiv \text{AlOH}$ functional groups on pedogenic Fe/Al (hydr)oxides. Because PO_4^{3-} and AsO_4^{3-} are iso-structural tetraoxoanions, phosphate displaces pre-adsorbed arsenate through ligand-exchange reactions, thereby increasing the dissolved fraction of As(V). This mechanism is well-documented in compost-amended contaminated soils (Cao et al., 2003). One option to mitigate the increase in As mobility upon vermicompost application is to add, to the SV and SVD treatments, an Fe-based by-product capable of adsorbing arsenic (Nielsen et al., 2011; Osono and Katoh, 2021), without materially increasing the overall treatment cost.

Finally, it can be observed that the effect of dolomite residue is positive in terms of reducing As mobility because the SVD treatment mobilises less As than the SV treatment. This effect is most plausibly explained by the dolomitic residue: the amendment releases Ca^{2+} and Mg^{2+} , increasing ionic strength; once supersaturation is reached, sparingly soluble Ca/Mg-arsenate and Ca-phosphate phases precipitate, simultaneously withdrawing PO_4^{3-} and AsO_4^{3-} from solution (Moon et al., 2004). By immobilising part of the phosphate, the competitive pressure on adsorption sites diminishes, and the resulting increase in extractable As is therefore markedly lower than with vermicompost alone.

The PCA (Fig. 3) highlights the treatment-dependent shifts in metal mobility: the untreated control soil (S) occupies the quadrant associated with the greatest geochemical risk for Cu and Zn, a zone defined by high acidity and a low Ca/P ratio. The additions containing dolomite by-product (SD, SBD and SVD) shift decisively toward negative PC1 values due to their pronounced alkalinising effect and prove the most effective at immobilising Cu, reducing its TCLP-extractable concentration to < 10 mg/kg. Vermicompost-based formulations (SV, SVD) move upward along PC2; the extra phosphorus supplied by the organic amendment fosters competitive desorption of arsenate, generating a modest rise in mobile As, yet they still suppress Zn (< 65 mg/kg) and Cu (< 3 mg/kg). Finally, the biochar treatment (SB) delivers a mild pH increase, accompanied by a high P load, effectively lowering Zn (≈ 30 – 65 mg/kg) and maintaining Cu at trace levels, while keeping As below detection.

Components satisfying the Kaiser–Guttman criterion (eigenvalue > 1) were retained; PC1 and PC2 accounted for 53 % and 21 % of the total variance, respectively. Scores and loadings were visualised in a Gabriel biplot generated with matplotlib 3.9, and sample points were labelled according to treatment (S, SD, SB, SV, SBD, SVD).

3.3. Effect of the different treatments on *Lolium multiflorum*

3.3.1. *Lolium multiflorum* biomass

As shown in Fig. 4A, vegetation (*Lolium multiflorum*) failed to

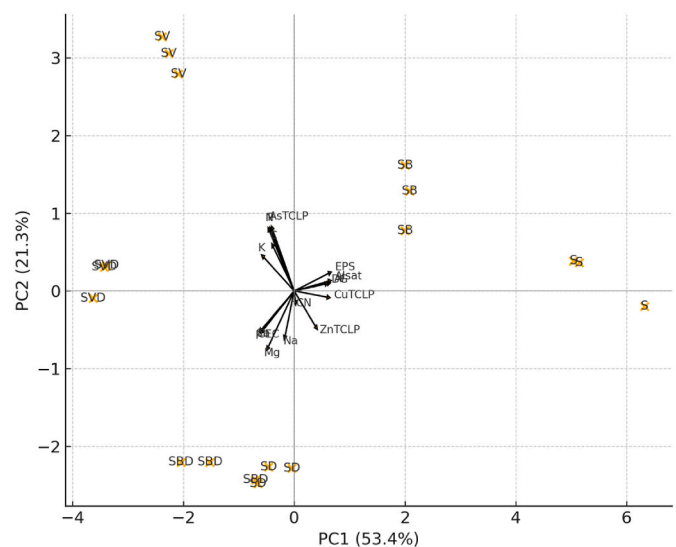


Fig. 3. Principal-component biplot depicting the ordination of the control soil and the five amended treatments together with the loadings of the studied variables. Treatment centroids are labelled; arrow length denotes the relative contribution of each variable to the two retained components. PCA = Principal component analysis, PC1 = first principal component, PC2 = second principal component. S = contaminated soil (negative control); SD = S + Dolomite by-product; SV = S + vermicompost; SB = S + biochar; SVD = S + vermicompost + dolomite by-product; SBD = S + biochar + dolomite by-product.

establish in soil S. This outcome is most plausibly attributable to the substrate's intrinsic constraints: an extremely low pH, elevated ESP, a high exchangeable-Al saturation, and excessive available Cu and Zn concentrations (Table S1).

Vegetation established under every amendment applied to soil S (even when the soil was treated only with the dolomitic residue, SD), highlighting the importance of correcting critical constraints such as pH, OC (except for SB treatment), ESP, exchangeable-Al saturation, and the excessive Cu and Zn available concentrations (Table 2; Fig. 2). These results concur with the findings reported by Forján et al. (2018b), Yang et al. (2016) and Zhao et al. (2018). Indeed, the present study revealed a significant correlation between OC and biomass ($r = 0.73$; $p < 0.01$) and between available Cu and biomass ($r = -0.63$; $p < 0.01$).

The highest biomass was recorded in the vermicompost-containing treatments (SV, SVD), as they not only alleviated the limitations discussed above but also produced the highest increases in soil N, P, and K (Table 2), all essential macronutrients for plant development (Cerqueira et al., 2022). These biomass gains under vermicompost-assisted treatments are consistent with prior reports in metal-impacted soils using vermicompost to support phytoextractors and improve post-remediation soil condition (Arai et al., 2001; Arai et al., 2001). In addition, SV and SVD treatments produced the most pronounced reductions in extractable Zn, which influences production (Kumar et al., 2018) (Fig. 4B).

3.3.2. Concentrations and harvested contents of Cu and Zn in *Lolium multiflorum*

Regarding the concentrations of Cu and Zn in the harvested vegetation, the SV treatment produced the highest concentrations of both Cu and Zn (Fig. 4B and C). *Lolium multiflorum* from SV also yielded the greatest biomass and the highest harvested loads of Cu and Zn (Table 3), confirming that this treatment offered more favourable growth conditions. Consequently, *Lolium multiflorum* accumulated higher Cu and Zn concentrations and showed an enhanced capacity for concentration, without evident negative effects. In the remaining treatments, no significant differences were detected in either the biomass concentrations of Cu and Zn (Fig. 2B and C) or the harvested Cu and Zn contents (Table 3).

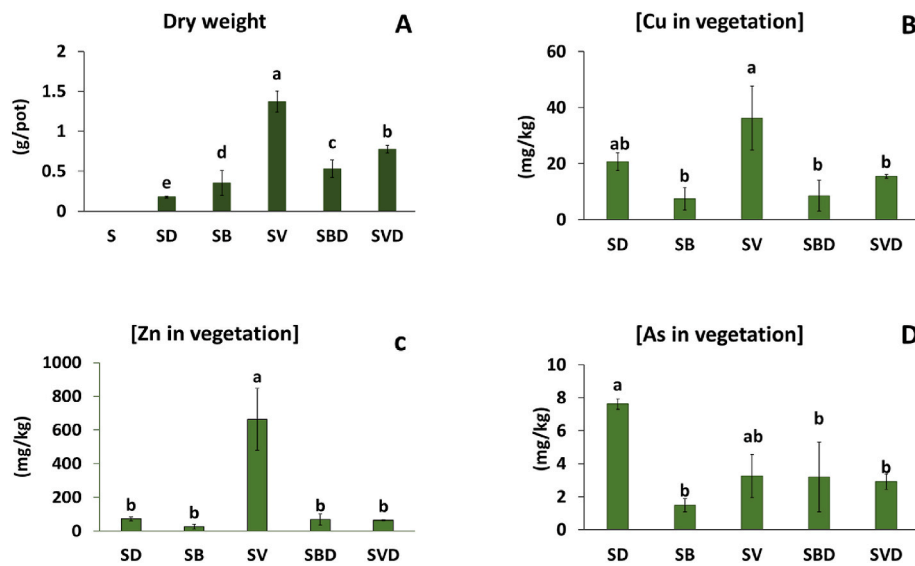


Fig. 4. A: Dry shoot biomass of *Lolium multiflorum* under each treatment; no growth was observed in the control. B: Copper (Cu) concentration in the biomass. C: Zinc (Zn) concentration in the biomass. D: Arsenic (As) concentration in the biomass. Different letters in different samples indicate significant differences ($n = 3$, ANOVA; $p < 0.05$). Error bars represent standard deviation. S = contaminated soil (negative control); SD = S + Dolomite by-product; SV = S + vermicompost; SB = S + biochar; SVD = S + vermicompost + dolomite by-product; SBD = S + biochar + dolomite by-product.

Table 3

Copper (Cu), zinc (Zn) and arsenic (As) contents were harvested from each pot (data for the control are omitted because no vegetation established) and the Bioconcentration Factor (BF) in *Lolium multiflorum* grown under each treatment.

		SD	SB	SV	SBD	SVD
Harvested (mg/pot)	Cu	3.81 ± 0.94b	1.50 ± 0.91b	45.99 ± 22.25a	4.24 ± 1.45b	11.89 ± 0.74b
	Zn	13.32 ± 3.50b	5.24 ± 2.81b	832.20 ± 520.55a	29.28 ± 7.99b	49.70 ± 1.81b
	As	1.17 ± 0.55b	0.37 ± 0.25b	3.35 ± 2.66a	1.57 ± 0.66b	2.26 ± 0.48 ab
BF	Cu	3.72 ± 0.44b	1.18 ± 0.58b	16.67 ± 10.55a	2.64 ± 2.86b	5.95 ± 0.49b
	Zn	0.78 ± 0.12b	0.52 ± 0.13b	10.61 ± 7.18a	0.73 ± 0.62b	3.92 ± 1.07b
	As	0	0	0.81 ± 0.58b	0	2.03 ± 0.41a

For each row, different letters in different samples mean significant differences ($n = 3$, ANOVA; $p < 0.05$). Typical deviation is represented by \pm . S = contaminated soil (negative control); SD = S + Dolomite by-product; SV = S + vermicompost; SB = S + biochar; SVD = S + vermicompost + dolomite by-product; SBD = S + biochar + dolomite by-product.

The response of the vegetation to As differed from that observed for Cu and Zn (Fig. 4C). *Lolium multiflorum* grown in soil amended exclusively with dolomitic residue (SD) exhibited the highest As concentrations, followed by plants grown under the SV treatment (Fig. 4C). Nevertheless, the greatest harvested As load occurred in the SV treatment (Table 3). This outcome is attributed to the more vigorous growth achieved under SV; indeed, a significant positive correlation was detected between total biomass and harvested As (0.80, $p < 0.01$).

3.3.3. Bioconcentration factor (BF)

The SV treatment had the highest bioconcentration factors (BF) for both Cu and Zn, indicating that vegetation grown in vermicompost-amended soil was physiologically healthier and therefore capable of accumulating greater amounts of Cu and Zn while achieving superior biomass production relative to the control and all other treatments (Table 4). This effect is probably linked to the more vigorous growth of *Lolium multiflorum* achieved under the SV and SVD treatments, as, in the rhizosphere, *Lolium multiflorum* releases root exudates that transiently modify the local pH and disrupt organomineral complexes (mineral-associated organic matter, MAO), thereby enhancing nutrient acquisition (Bölscher et al., 2025). These interactions can simultaneously mobilise metallic cations; in this context, it is worth recalling that Cu and Zn function as essential plant micronutrients (Tao et al., 2004).

The only treatments for which a bioconcentration factor (BF) for As could be computed were SV and SVD (Table 3), and even in these cases the BF values were low. This finding is consistent with the fact that

available As was detectable exclusively in those two treatments and that these two treatments had the highest *Lolium multiflorum* biomass (Fig. 4A–C). Significantly positive correlations were observed between BF and harvested biomass (0.53, $p < 0.01$) and between BF and available As concentrations (0.65, $p < 0.01$).

3.4. Carbon sequestration

Carbon sequestration in this experiment reflects a balance between the amount of new carbon added or fixed and the efficiency with which that carbon is stabilised (Fig. 5).

Biochar stands out for contributing large quantities of chemically recalcitrant carbon (Forján et al., 2018b). In contrast, vermicompost is particularly effective in stimulating root-derived carbon inputs and the formation of mineral-associated organic matter (MAO) under alkaline conditions (Vidal et al., 2020).

However, in this study, the SV treatment exhibited the highest sequestered carbon content, followed by SB, SBD, and SVD, with the lowest values recorded in S and SD (Fig. 5). The dolomite by-product alone (SD) lacks sufficient organic carbon. When combined with other amendments, it partially dilutes and accelerates the mineralisation of labile fractions, resulting in intermediate carbon sequestration. It is essential to recognise that a substantial portion of soil organic carbon originates from rhizodeposition, comprising soluble root exudates, sloughed cortical cells, and the necromass of root-associated microorganisms (Bölscher et al., 2025). In the present study, the highest carbon

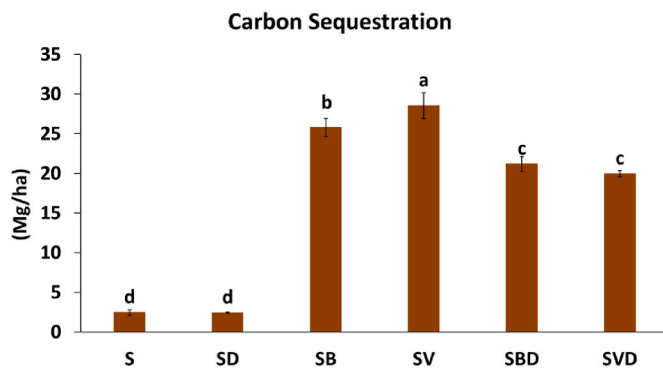


Fig. 5. Carbon sequestration in the soil S and in the different treatments. Different letters in different samples indicate significant differences ($n = 3$, ANOVA; $p < 0.05$). Error bars represent standard deviation.

sequestration values were recorded in the treatments that promoted the most vigorous growth of *Lolium multiflorum* (SV, SVD) (Fig. 4A and 5), highlighting a strong functional link between plant productivity and below-ground carbon accumulation. Indeed, a significantly positive correlation was observed between harvested biomass and sequestered carbon in these treatments ($r = 0.89$, $p < 0.05$).

4. Conclusions

Our results support the initial hypothesis that dolomite by-product (D)—particularly when co-applied with vermicompost (VC)—can simultaneously neutralise severe soil acidity, immobilise toxic metal (loid)s, and enhance phytostabilisation potential. Applied alone, D rapidly increased soil pH from 3.03 to >8.3 , reduced exchangeable Al^{3+} to negligible levels, and created conditions favourable for plant establishment. In parallel, As mobility decreased, most plausibly via precipitation and/or co-precipitation of sparingly soluble Ca/Mg arsenate, carbonate, and hydroxide phases.

When combined with VC, remediation performance was maximized: CEC increased, soil fertility indicators improved, $>90\%$ of bioavailable Cu and Zn were immobilised, and *Lolium multiflorum* achieved the highest biomass. By contrast, VC alone tended to increase extractable As—consistent with phosphate competition and DOC-mediated desorption—although co-application with D mitigated this effect relative to VC alone. The D + biochar (B) mixture improved pH and CEC but was less effective for Zn and appeared to accelerate mineralisation of labile C, limiting net C gains.

Overall, integrating D with VC emerges as a scalable, low-impact, circular, nature-based solution that valorises an industrial residue while rehabilitating degraded, metal-contaminated soils and contributing to climate-smart land management.

CRedit authorship contribution statement

Lorena Salgado: Writing – original draft, Software, Investigation, Formal analysis. **José Luis R. Gallego:** Writing – review & editing, Supervision, Funding acquisition, Conceptualization. **Roberto Caballero:** Visualization, Conceptualization. **María Larramona:** Investigation, Formal analysis. **Elias Afif:** Formal analysis, Data curation. **Maximino Herías:** Visualization, Investigation, Formal analysis. **Raquel Lara:** Formal analysis, Data curation. **Juan María Menéndez-Aguado:** Writing – original draft, Visualization. **Rubén Forján:** Writing – original draft, Visualization, Software, Methodology, Investigation, Data curation, Conceptualization.

Funding

This project was funded by the INTERSOIL project

(PID2023–147718NB-I00, AEI/Spain, FEDER/EU) and by the project IDE/2023/000423, SEKUENS Agency, Asturias, Spain.

Declaration of competing interest

The authors declare the following financial interests/personal relationships which may be considered as potential competing interests: J. R. Gallego reports financial support was provided by State Agency of Research Spain. J. R. Gallego reports financial support was provided by SEKUENS Agency. If there are other authors, they declare that they have no known competing financial interests or personal relationships that could have appeared to influence the work reported in this paper.

Acknowledgements

Intocast Ibérica SL acknowledges the team's scientific contribution, whose expertise and collaboration were essential to addressing industrial and environmental challenges and advancing sustainable practices.

Appendix A. Supplementary data

Supplementary data to this article can be found online at <https://doi.org/10.1016/j.jenvman.2025.127795>.

Data availability

Data will be made available on request.

References

- Ahmad, M., Rajapaksha, A.U., Lim, J.E., Zhang, M., Bolan, N., Mohan, D., Vithanage, M., Lee, S.S., Ok, Y.S., 2014. Biochar as a sorbent for contaminant management in soil and water: a review. *Chemosphere* 99, 19–33. <https://doi.org/10.1016/j.chemosphere.2013.10.071>.
- Anta, R., Calvo, E., Sabarís, F., Costa, J., Mosquera, N., Macías Vázquez, F., Camps-Arbestain, M., García, N., 2015. Soil organic carbon in northern Spain (Galicia, Asturias and País Vasco). *Spanish J. Soil Sci.* 5, 41–53. <https://doi.org/10.3232/SJSS.2015.V5.N1.04>.
- Arai, Y., Elzinga, E.J., Sparks, D.L., 2001. X-ray absorption spectroscopic investigation of arsenite and arsenate adsorption at the aluminum oxide–water interface. *J. Colloid Interface Sci.* 235, 80–88. <https://doi.org/10.1006/JCIS.2000.7249>.
- Arwenyo, B., Varco, J.J., Dygert, A., Brown, S., Pittman, C.U., Mlnsa, T., 2023. Contribution of modified P-enriched biochar on pH buffering capacity of acidic soil. *J. Environ. Manag.* 339, 117863. <https://doi.org/10.1016/J.JENVMAN.2023.117863>.
- Baragaño, D., José, J.L., Forján, R., 2021. Short-term experiment for the in situ stabilisation of a polluted soil using mining and biomass waste. *J. Environ. Manag.* 296, 113179. <https://doi.org/10.1016/j.jenvman.2021.113179>.
- Bolan, N., Sarmah, A.K., Bordoloi, S., Bolan, S., Padhye, L.P., Van Zwieten, L., Sooriyakumar, P., Khan, B.A., Ahmad, M., Solaiman, Z.M., Rinklebe, J., Wang, H., Singh, B.P., Siddique, K.H.M., 2023. Soil acidification and the liming potential of biochar. *Environ. Pollut.* 317, 120632. <https://doi.org/10.1016/J.ENVPOL.2022.120632>.
- Bölscher, T., Cardon, Z.G., García Arredondo, M., Grand, S., Griffen, G., Hestrin, R., Imboden, J., Jamoteau, F., Lacroix, E.M., Pérez Castro, S., Persson, P., Riley, W.J., Keilueit, M., 2025. Vulnerability of mineral-organic associations in the rhizosphere. *Nat. Commun.* 16, 5527. <https://doi.org/10.1038/s41467-025-61273-4>.
- Calvo, R.M., Macías Vázquez, F., Buurman, P., 1987. Procesos de alteración y neoformación mineral en medios serpentínicos de Galicia. *Cuad. do Lab. Xeolóxico Laxe* 11, 161–170.
- Cañedo-Argüelles, M., Kefford, B.J., Piscart, C., Prat, N., Schäfer, R.B., Schulz, C.J., 2013. Salinisation of rivers: an urgent ecological issue. *Environ. Pollut.* 173, 157–167. <https://doi.org/10.1016/J.ENVPOL.2012.10.011>.
- Cao, X., Ma, L.Q., Shiralipour, A., 2003. Effects of compost and phosphate amendments on arsenic mobility in soils and arsenic uptake by the hyperaccumulator, *Pteris vittata* L. *Environ. Pollut.* 126, 157–167. [https://doi.org/10.1016/S0269-7491\(03\)00208-2](https://doi.org/10.1016/S0269-7491(03)00208-2).
- Cerdeira-Pérez, A., Monterroso, C., Rodríguez-Garrido, B., Machinet, G., Echevarria, G., Prieto-Fernández, Á., Kidd, P.S., 2019. Implementing nickel phytomining in a serpentine quarry in NW Spain. *J. Geochem. Explor.* 197, 1–13. <https://doi.org/10.1016/J.GEXPLO.2018.11.001>.
- Cerqueira, B., Covelo, E.F., Rúa-Díaz, S., Marcet, P., Forján, R., Gallego, J.L.R., Trakal, L., Beesley, L., 2022. Contrasting mobility of arsenic and copper in a mining soil: a comparative column leaching and pot testing approach. *J. Environ. Manag.* 318, 115530. <https://doi.org/10.1016/J.JENVMAN.2022.115530>.

- Chalot, M., 2024. Phytomanagement as a Nature-based Solution for Polluted Soils. (*Advances in Botanical Research*, 109. Academic Press (Elsevier). ISBN:978-0-443-15825-4.
- Chunwichit, S., Phusantisampan, T., Thongchai, A., Taeprayoon, P., Pechampai, N., Kubola, J., Pichtel, J., Meeinkuir, W., 2024. Influence of soil amendments on phytostabilisation, localisation and distribution of zinc and cadmium by marigold varieties. *Sci. Total Environ.* 919, 170791. <https://doi.org/10.1016/J.SCITOTENV.2024.170791>.
- de Oliveira Paiva, I., de Moraes, E.G., Jindo, K., Silva, C.A., 2024. Biochar N content, pools and aromaticity as affected by feedstock and pyrolysis temperature. *Waste and Biomass Valor.* 15, 3599–3619. <https://doi.org/10.1007/S12649-023-02415-X>.
- Ding, X., Li, G., Zhao, X., Lin, Q., Wang, X., 2023. Biochar application significantly increases soil organic carbon under conservation tillage: an 11-year field experiment. *Biochar* 5, 1–14. <https://doi.org/10.1007/S42773-023-00226-W>.
- European Commission, 2017. Nature-based solutions [WWW Document]. https://research-and-innovation.ec.europa.eu/research-area/environment/nature-based-solutions_en.
- European Commission, 2014. Towards a circular economy: A zero waste programme for Europe [WWW Document]. Commun. from Comm. to Eur. Parliam. Counc. Eur. Econ. Soc. Comm. Comm. regions.
- European Commission, 2020. Communication From The Commission To The European Parliament, The Council, The European Economic And Social Committee And The Committee Of The Regions Stepping up Europe's 2030 Climate Investing in a climate-neutral Future for the Benefit of our People am.
- Fang, H., Zhou, C., Guan, D.X., Azeem, M., Li, G., 2025. Synergistic approaches for sustainable remediation of organic contaminated soils: integrating biochar and phytoremediation. *Agriculture* 15 (8), 905. <https://doi.org/10.3390/AGRICULTURE15080905>.
- Fiorentino, A., Rajput, F.Z., Di Serio, A., Baldi, V., Guarino, F., Baldantoni, D., Ronga, D., Mazzei, P., Motta, O., Falanga, M., Ciatelli, A., Castiglione, S., 2025. Role of plants and urban soils in carbon stock: status, modulators, and sustainable management practices. *Plants* 14 (4), 546. <https://doi.org/10.3390/PLANTS14040546>.
- Forján, R., Arias-Estévez, M., Gallego, J.L.R., Santos, E., Arenas-Lago, D., 2024. Biochar-nanoparticle combinations enhance the biogeochemical recovery of a post-mining soil. *Sci. Total Environ.* 930, 172451. <https://doi.org/10.1016/J.SCITOTENV.2024.172451>.
- Forján, R., Rodríguez-Vila, A., Cerqueira, B., Covelo, E.F., 2018a. Effects of compost and technosol amendments on metal concentrations in a mine soil planted with *Brassica juncea* L. *Environ. Sci. Pollut. Res.* 25, 19713–19727. <https://doi.org/10.1007/s11356-018-2173-1>.
- Forján, R., Rodríguez-Vila, A., Covelo, E.F., 2018b. Using compost and technosol combined with biochar and *Brassica juncea* L. to decrease the bioavailable metal concentration in soil from a copper mine settling pond. *Environ. Sci. Pollut. Res.* 25, 1294–1305. <https://doi.org/10.1007/s11356-017-0559-0>.
- Formentini, T.A., Fekiacova-Castanet, Z., Pinheiro, A., Doelsch, E., 2025. Unique behavior of zinc in organic waste-amended soils: a review bridging molecular processes and environmental fate. *Environ. Pollut.* 377, 126459. <https://doi.org/10.1016/J.ENVPOL.2025.126459>.
- Garbus, S., Mackay, A., Camps-Arbestain, M., DeVantier, B., Minor, M., 2021. Biochar amendment improves soil physico-chemical properties and alters root biomass and the soil food web in grazed pastures. *Agric. Ecosyst. Environ.* 319, 107517. <https://doi.org/10.1016/J.AGEE.2021.107517>.
- García-Montero, L.G., Valverde-Aseño, I., Grande-Ortiz, M.A., Menta, C., Hernandez, L., 2013. Impact of earthworm casts on soil pH and calcium carbonate in black truffle burns. *Agrofor. Syst.* 87, 815–826. <https://doi.org/10.1007/S10457-013-9598-9>.
- Gebreikidan, A., Weldegebriel, Y., Hadera, A., Van der Bruggen, B., 2013. Toxicological assessment of heavy metals accumulated in vegetables and fruits grown in Ginfel river near Sheba Tannery, Tigray, Northern Ethiopia. *Ecotoxicol. Environ. Saf.* 95, 171–178. <https://doi.org/10.1016/J.ECOENV.2013.05.035>.
- Geng, N., Kang, X., Yan, X., Yin, N., Wang, H., Pan, H., Yang, Q., Lou, Y., Zhuge, Y., 2022. Biochar mitigation of soil acidification and carbon sequestration is influenced by materials and temperature. *Ecotoxicol. Environ. Saf.* 232, 113241. <https://doi.org/10.1016/J.ECOENV.2022.113241>.
- Hazleton, P., Murphy, B., 2007. Interpreting soil Test results: what do all the numbers mean? Interpreting Soil Test Results. CSIRO Publishing. <https://doi.org/10.1071/9780643094680>.
- Hendershot, W.H., Duquette, M., 1986. A simple barium chloride method for determining cation exchange capacity and exchangeable cations. *Soil Sci. Soc. Am. J.* 50, 605–608. <https://doi.org/10.2136/sssaj1986.0361599500500030013x>.
- Houba, V.J.G., Temminghoff, E.J.M., Gaikhorst, G.A., van Vark, W., 2008. Soil analysis procedures using 0.01 M calcium chloride as extraction reagent. *Commun. Soil Sci. Plant Anal.* 31, 1299–1396. <https://doi.org/10.1080/00103620009370514>.
- Hütsch, B.W., Augustin, J., Merbach, W., 2002. Plant rhizodeposition — an important source for carbon turnover in soils. *J. Plant Nutr. Soil Sci.* 165, 397–407. <https://doi.org/10.1016/j.still.2025.106726>.
- Ingvar Nilsson, S., Andersson, S., Valeur, I., Persson, T., Bergholm, J., Wirén, A., 2001. Influence of dolomitic lime on leaching and storage of C, N and S in a Spodosol under Norway spruce (*Picea abies* (L.) Karst.). *For. Ecol. Manage.* 146, 55–73. [https://doi.org/10.1016/S0378-1127\(00\)00452-7](https://doi.org/10.1016/S0378-1127(00)00452-7).
- International Organization for Standardization, 2020. Particle size analysis — Laser diffraction methods (ISO 13320:2020).
- Islas-Valdez, S., Lucho-Constantino, C.A., Beltrán-Hernández, R.I., Gómez-Mercado, R., Vázquez-Rodríguez, G.A., Herrera, J.M., Jiménez-González, A., 2017. Effectiveness of rabbit manure biofertiliser in barley crop yield. *Environ. Sci. Pollut. Res.* 24, 25731–25740. <https://doi.org/10.1007/S11356-015-5665-2>.
- Kafle, A., Timilsina, A., Gautam, A., Adhikari, K., Bhattarai, A., Aryal, N., 2022. Phytoremediation: mechanisms, plant selection and enhancement by natural and synthetic agents. *Environ. Adv.* 8, 100203. <https://doi.org/10.1016/J.ENVADV.2022.100203>.
- Kameda, K., Hashimoto, Y., Ok, Y.S., 2018. Stabilisation of arsenic and lead by magnesium oxide (MgO) in different seawater concentrations. *Environ. Pollut.* 233, 952–959. <https://doi.org/10.1016/J.ENVPOL.2017.09.067>.
- Kossoff, D., Dubbin, W.E., Alfredsson, M., Edwards, S.J., Macklin, M.G., Hudson-Edwards, K.A., 2014. Mine tailings dams: characteristics, failure, environmental impacts, and remediation. *Appl. Geochem.* 51, 229–245. <https://doi.org/10.1016/J.APGEOCHEM.2014.09.010>.
- Kumar, A., Tsechansky, L., Lew, B., Raveh, E., Frenkel, O., Graber, E.R., 2018. Biochar alleviates phytotoxicity in *Ficus elastica* grown in Zn-contaminated soil. *Sci. Total Environ.* 618, 188–198. <https://doi.org/10.1016/J.SCITOTENV.2017.11.013>.
- Ladeira, A.C.Q., Ciminelli, V.S.T., 2004. Adsorption and desorption of arsenic on an oxisol and its constituents. *Water Res.* 38, 2087–2094. <https://doi.org/10.1016/J.WATRES.2004.02.002>.
- Lanas, J., Alvarez, J.I., 2004. Dolomitic limes: evolution of the slaking process under different conditions. *Thermochim. Acta* 423, 1–12. <https://doi.org/10.1016/J.TCA.2004.04.016>.
- Lenton, T.M., 2010. The potential for land-based biological CO2 removal to lower future atmospheric CO2 concentration. *Carbon Manag.* 1, 145–160. <https://doi.org/10.4155/CM.T.10.12>.
- Lin, W., Zhou, F., Luo, W., You, L., 2021. Recycling the waste dolomite powder with excellent consolidation properties: sample synthesis, mechanical evaluation, and consolidation mechanism analysis. *Constr. Build. Mater.* 290, 123198. <https://doi.org/10.1016/J.CONBUILDMAT.2021.123198>.
- Liu, S., Cen, B., Yu, Z., Qiu, R., Gao, T., Long, X., 2025. The key role of biochar in amending acidic soil: reducing soil acidity and improving soil acid buffering capacity. *Biochar* 7, 52. <https://doi.org/10.1007/S42773-025-00432-8>.
- Lou, X.F., Nair, J., 2009. The impact of landfilling and composting on greenhouse gas emissions – a review. *Bioresour. Technol.* 100, 3792–3798. <https://doi.org/10.1016/J.BIORTECH.2008.12.006>.
- Macías Vázquez, F., Calvo de Anta, R.M., 1983. El análisis del medio físico y su aplicación a la ordenación del territorio: una experiencia piloto en el área de Padrón. *Trab. Compostelanos Biol.* 10, 179–208.
- Malal, H., Romero, V.S., Horwath, W.R., Dore, S., Beckett, P., Ait Hamza, M., Lakhtar, H., Lazcano, C., 2024. Vermifiltration and sustainable agriculture: unveiling the soil health-boosting potential of liquid waste vermicompost. *Front. Sustain. Food Syst.* 8, 1383715. <https://doi.org/10.3389/FSUFS.2024.1383715>.
- Martin, N., Le Guet, T., Dupuy, F., Grybos, M., Joussein, E., 2024. Effect of liming on polycyclic aromatic hydrocarbons leaching from hydrocarbon-contaminated tectogenic industriosoil. *Environ. Pollut.* 351, 124063. <https://doi.org/10.1016/J.ENVPOL.2024.124063>.
- Masini, J.C., Abate, G., Lima, E.C., Hahn, L.C., Nakamura, M.S., Lichtig, J., Nagatomi, H. R., 1998. Comparison of methodologies for determination of carboxylic and phenolic groups in humic acids. *Anal. Chim. Acta* 364, 223–233. [https://doi.org/10.1016/S0003-2670\(98\)00045-2](https://doi.org/10.1016/S0003-2670(98)00045-2).
- Mehlich, A., 1984. Mehlich 3 soil test extractant: a modification of Mehlich 2 extractant. *Commun. Soil Sci. Plant Anal.* 15, 1409–1416. <https://doi.org/10.1080/00103628409367568>.
- Mesquita, M.E., Vieira E Silva, J.M., 1996. Zinc adsorption by a calcareous soil. Copper interaction. *Geoderma* 69, 137–146. [https://doi.org/10.1016/0016-7061\(95\)00058-5](https://doi.org/10.1016/0016-7061(95)00058-5).
- Moon, D.H., Dermatas, D., Menounou, N., 2004. Arsenic immobilisation by calcium-arsenic precipitates in lime treated soils. *Sci. Total Environ.* 330, 171–185. <https://doi.org/10.1016/J.SCITOTENV.2004.03.016>.
- Pang, D., Xu, H., 2024. Carbon sequestration and stability and soil erosion in Forest ecosystems. *Forests* 15, 1961. <https://doi.org/10.3390/F15111961>.
- Patel, K., Vashist, M., Goyal, D., Sarma, R., Garg, R., Singh, S.K., 2025. From waste to resource: a life cycle assessment of biochar from agricultural residue. *Environ. Prog. Sustain. Energy* 44, e14558. <https://doi.org/10.1002/EP.14558>.
- Phillips, C.L., Meyer, K.M., Garcia-Jaramillo, M., Weidman, C.S., Stewart, C.E., Wanzek, T., Grusak, M.A., Watts, D.W., Novak, J., Trippe, K.M., 2022. Towards predicting biochar impacts on plant-available soil nitrogen content. *Biochar* 4, 1–15. <https://doi.org/10.1007/S42773-022-00137-2>.
- Porta, J., 1986. Técnicas y Experimentos de Edafología. Coll. Of. D'enginyers Agron. Catalunya. Barcelona.
- Przemieniecki, S.W., Zapałowska, A., Skwiercz, A., Damszel, M., Telesiński, A., Sierota, Z., Gorczyca, A., 2021. An evaluation of selected chemical, biochemical, and biological parameters of soil enriched with vermicompost. *Environ. Sci. Pollut. Res.* 28, 8117–8127. <https://doi.org/10.1007/S11356-020-10981-Z>.
- Rinklebe, J., Shaheen, S.M., Frohne, T., 2016. Amendment of biochar reduces the release of toxic elements under dynamic redox conditions in a contaminated floodplain soil. *Chemosphere* 142, 41–47. <https://doi.org/10.1016/J.CHEMOSPHERE.2015.03.067>.
- Rosenkranz, T., Hipfinger, C., Ridard, C., Puschenreiter, M., 2019. A nickel phytomining field trial using *odontarrhena chalcidica* and *Noccaea goesingensis* on an Austrian serpentine soil. *J. Environ. Manag.* 242, 522–528. <https://doi.org/10.1016/J.JENVMAN.2019.04.073>.
- Rúa-Díaz, S., Forján, R., Lago-Vila, M., Cerqueira, B., Arco-Lázaro, E., Marcet, P., Baragaño, D., José, Gallego, J.R., Covelo, E.F., 2023. Pyrolysis temperature influences the capacity of biochar to immobilise copper and arsenic in mining soil remediation. *Environ. Sci. Pollut. Res.* 32882–32893. <https://doi.org/10.1007/s11356-022-24492-6>.
- Salgado, L., López-Sánchez, C.A., Colina, A., Baragaño, D., Forján, R., Gallego, J.R., 2023. Hg and as pollution in the soil-plant system evaluated by combining

- multispectral UAV-RS, geochemical survey and machine learning. *Environ. Pollut.* 333, 122066. <https://doi.org/10.1016/j.envpol.2023.122066>.
- Sarma, B., Farooq, M., Gogoi, N., Borkotoki, B., Kataki, R., Garg, A., 2018. Soil organic carbon dynamics in wheat - green gram crop rotation amended with vermicompost and biochar in combination with inorganic fertilisers: a comparative study. *J. Clean. Prod.* 201, 471–480. <https://doi.org/10.1016/J.JCLEPRO.2018.08.004>.
- Singh, B.P., Cowie, A.L., 2014. Long-term influence of biochar on native organic carbon mineralisation in a low-carbon clayey soil. *Sci. Rep.* 4, 1–9. <https://doi.org/10.1038/srep03687>.
- Song, Y., Kirkwood, N., Maksimović, Č., Zhen, X., O'Connor, D., Jin, Y., Hou, D., 2019. Nature based solutions for contaminated land remediation and brownfield redevelopment in cities: a review. *Sci. Total Environ.* 663, 568–579. <https://doi.org/10.1016/J.SCITOTENV.2019.01.347>.
- Sweet, S.K., Bassuk, N.L., Miller, B.M., 2025. Deep compost amendment reduces soil bulk density resulting in improved growth of urban *Gymnocladus dioica* trees over time. *Urban For. Urban Green.* 108, 128822. <https://doi.org/10.1016/J.UFUG.2025.128822>.
- Tao, S., Liu, W.X., Chen, Y.J., Xu, F.L., Dawson, R.W., Li, B.G., Cao, J., Wang, X.J., Hu, J. Y., Fang, J.Y., 2004. Evaluation of factors influencing root-induced changes of copper fractionation in rhizosphere of a calcareous soil. *Environ. Pollut.* 129, 5–12. <https://doi.org/10.1016/J.ENVPOL.2003.10.001>.
- Terefe, Z., Feyisa, T., Molla, E., Ejigu, W., 2024. Effects of vermicompost and lime on acidic soil properties and malt barley (*Hordeum Distichum* L.) productivity in Mecha district, northwest Ethiopia. *PLoS One* 19, e0311914. <https://doi.org/10.1371/JOURNAL.PONE.0311914>.
- Trentin, E., Facco, D.B., Hammerschmitt, R.K., Avelar Ferreira, P.A., Morsch, L., Belles, S. W., Ricachenevsky, F.K., Nicoloso, F.T., Ceretta, C.A., Tiecher, T.L., Tarouco, C.P., Berghetti, Á.L.P., Toselli, M., Brunetto, G., 2019. Potential of vermicompost and limestone in reducing copper toxicity in young grapevines grown in Cu-contaminated vineyard soil. *Chemosphere* 226, 421–430. <https://doi.org/10.1016/J.CHEMOSPHERE.2019.03.141>.
- Ursueguía, D., Faba, L., Díaz, E., Caballero, R., Ordóñez, S., 2023. Dolomite industrial byproducts as active material for CO₂ adsorption and catalyst for the acetone condensation. *Waste Manag.* 168, 431–439. <https://doi.org/10.1016/J.WASMAN.2023.06.031>.
- USEPA, 1992. SW-846 Test Method 1311: Toxicity Characteristic Leaching Procedure.
- Van Bemmelen, J.M., 1890. Über die Bestimmung des Wassers, des Humus, des Schwefels, der in den colloidalen Silikaten gebundenen Kieselsäure, des Mangans usw im Ackerboden. *Die Landwirtschaftlichen Versuchs-Stationen* 37, e290.
- Varol, M., 2011. Assessment of heavy metal contamination in sediments of the Tigris River (Turkey) using pollution indices and multivariate statistical techniques. *J. Hazard. Mater.* 195, 355–364. <https://doi.org/10.1016/J.JHAZMAT.2011.08.051>.
- Verheijen, F.G.A., Zhuravel, A., Silva, F.C., Amaro, A., Ben-Hur, M., Keizer, J.J., 2019. The influence of biochar particle size and concentration on bulk density and maximum water holding capacity of sandy vs sandy loam soil in a column experiment. *Geoderma* 347, 194–202. <https://doi.org/10.1016/J.GEODERMA.2019.03.044>.
- Vidal, A., Lenhart, T., Dignac, M.F., Biron, P., Höschel, C., Barthod, J., Vedere, C., Vaury, V., Bariac, T., Rumpel, C., 2020. Promoting plant growth and carbon transfer to soil with organic amendments produced with mineral additives. *Geoderma* 374, 114454. <https://doi.org/10.1016/J.GEODERMA.2020.114454>.
- Vrinceanu, N.O., Motelică, D.M., Dumitru, M., Calciu, I., Tănase, V., Preda, M., 2019. Assessment of using bentonite, dolomite, natural zeolite and manure for the immobilisation of heavy metals in a contaminated soil: the Copșa Mică case study (Romania). *Catena* 176, 336–342. <https://doi.org/10.1016/J.CATENA.2019.01.015>.
- Wang, F., Zhang, W., Miao, L., Ji, T., Wang, Y., Zhang, H., Ding, Y., Zhu, W., 2021. The effects of vermicompost and shell powder addition on Cd bioavailability, enzyme activity and bacterial community in Cd-contaminated soil: a field study. *Ecotoxicol. Environ. Saf.* 215, 112163. <https://doi.org/10.1016/J.ECOENV.2021.112163>.
- Wang, H.B., Liu, X.P., Jin, B.J., Shu, Y.C., Sun, C.L., Zhu, Y.G., Lin, X.Y., 2024. High-molecular-weight dissolved organic matter enhanced phosphorus availability in paddy soils: evidence from field and microcosm experiments. *Soil Tillage Res.* 240, 106099. <https://doi.org/10.1016/J.STILL.2024.106099>.
- Waychunas, G.A., Rea, B.A., Fuller, C.C., Davis, J.A., 1993. Surface chemistry of ferrihydrite: part 1. EXAFS studies of the geometry of coprecipitated and adsorbed arsenate. *Geochem. Cosmochim. Acta* 57, 2251–2269. [https://doi.org/10.1016/0016-7037\(93\)90567-G](https://doi.org/10.1016/0016-7037(93)90567-G).
- Wong, M.H., 2003. Ecological restoration of mine degraded soils, with emphasis on metal contaminated soils. *Chemosphere* 50, 775–780. [https://doi.org/10.1016/S0045-6535\(02\)00232-1](https://doi.org/10.1016/S0045-6535(02)00232-1).
- Worlanyo, A.S., Jiangfeng, L., 2021. Evaluating the environmental and economic impact of mining for post-mined land restoration and land-use: a review. *J. Environ. Manag.* 279, 111623. <https://doi.org/10.1016/J.JENVMAN.2020.111623>.
- Wu, H., Hu, J., Shaaban, M., Xu, P., Zhao, J., Hu, R., 2021. The effect of dolomite amendment on soil organic carbon mineralisation is determined by the dolomite size. *Ecol. Process.* 10, 1–12. <https://doi.org/10.1186/S13717-020-00278-X>.
- Yang, S.X., Liao, B., Yang, Z.H., Chai, L.Y., Li, J.T., 2016. Revegetation of extremely acid mine soils based on aided phytostabilisation: a case study from southern China. *Sci. Total Environ.* 562, 427–434. <https://doi.org/10.1016/J.SCITOTENV.2016.03.208>.
- Zhao, Y., Wang, S., Li, Y., Liu, J., Zhuo, Y., Chen, H., Wang, J., Xu, L., Sun, Z., 2018. Extensive reclamation of saline-sodic soils with flue gas desulfurisation gypsum on the Songnen Plain, Northeast China. *Geoderma* 321, 52–60. <https://doi.org/10.1016/J.GEODERMA.2018.01.033>.